DISTRIBUTED PATH OPTIMIZATION OF MULTIPLE UAVS FOR AOA TARGET LOCALIZATION

Sheng Xu[⋆a], *Kutluyıl Doğançay*[⋆◇a] *and Hatem Hmam*[b]

[⋆]Institute for Telecommunications Research, [◇]School of Engineering
[a]University of South Australia, Australia
[b]Cyber and Electronic Warfare Division, DST Group, Australia

ABSTRACT

This paper is concerned with unmanned aerial vehicle (UAV) path optimization for AOA target localization via distributed processing. A distributed UAV path optimization algorithm based on gradient descent method is developed using the diffusion extended Kalman filter (DEKF). With this algorithm, a group of UAVs can realize self-adaptive path optimization in order to improve estimation performance. The presented distributed path optimization strategy aims to minimize the estimation mean squared error (MSE) by minimizing the trace of the error covariance matrix. The UAV dynamic communication topology caused by communication range constraint is analyzed. Furthermore, the UAV 6-degree-of-freedom (DOF) dynamic modeling is taken into consideration to generate realistic UAV trajectories. The properties and effectiveness of the proposed algorithm are discussed and verified with simulation examples.

***Index Terms*—** Unmanned aerial vehicle (UAV), angle-of-arrival localization, diffusion extended Kalman filter, distributed path optimization.

1. INTRODUCTION

In recent years unmanned aerial vehicles (UAVs) have been widely used for target localization employing angle-of-arrival (AOA) sensors [1, 2]. In AOA target localization, the target location is determined by triangulation of the angle measurements collected by multiple UAVs. The path of each UAV plays a vital role in determining target localization performance [3].

AOA target localization with optimal path planned UAV has been an active research area. In [4], a gradient descent optimal path planning method was proposed in order to minimize the estimation mean squared error (MSE) for AOA target localization. By maximizing the determinant of Fisher information matrix (FIM), [5] proposed an optimal AOA sensor trajectory planning method using a single mobile sensor. In [6], the gradient descent method was improved by solving a nonlinear programming problem over discrete UAV waypoints. For multiple sensors, [7] and [8] presented different optimal sensor deployment strategies for AOA target localization by maximizing the determinant of the FIM in 2D and 3D, respectively. In [9], an optimal sensor deployment strategy was proposed for a static target localization in 3D assuming multiple sensors with identical elevation angles from the target. However, for a group of distributed mobile sensors, few works have tackled the distributed path optimization problem for AOA target localization.

Using multiple sensors has advantages on estimation accuracy and system reliability, and becomes a good choice for AOA target localization. The distributed estimation strategy has many advantages compared with centralized estimation: (1) it has low-energy communication requirement, (2) it allows parallel processing, (3) every UAV becomes independent and robust to link failure problem [10, 11, 12]. However, as the information acquired by each UAV is limited, the estimation accuracy will decrease.

In this paper, we focus on distributed UAV path optimization for AOA target localization. The UAV 6-DOF dynamic modeling is considered and a diffusion extended Kalman filter (DEKF) is used to implement distributed adaptive estimation. A distributed UAV path optimization algorithm based on gradient descent method is proposed. The dynamic communication topology caused by communication distance limitation is considered. The paper is organized as follows. Section 2 describes the UAV 6-DOF dynamic modeling. The DEKF for AOA target localization is developed in Section 3. The distributed UAV path optimization algorithm is designed in Section 4. Communication topology and complexity are analyzed in Section 5. Simulation results are presented in Section 6. Section 7 draws the conclusion.

2. 6-DOF UAV DYNAMIC MODEL

In real-life applications, fixed-wing UAVs can hardly arrive at the waypoints given by high-level commands because of the influences of 6-DOF dynamic model. In order to obtain accurate UAV flying trajectories we propose a fixed-wing UAV 6-DOF model which will be used in path optimization.

The parameters for the UAV 6-DOF dynamic model are roll angle φ, pitch angle Θ and yaw angle ψ [13]. Roll, pitch and yaw angular velocities are p, q and r, respectively. The total forces along three axes are F_x, F_y, F_z and the total moments are M_x, M_y, M_z. The equations of UAV translation in the earth coordinates can be written as:

$$\begin{aligned} F_x &= m(\dot{U} - rV + qW) - mg\sin\Theta \\ F_y &= m(\dot{V} - pW + rU) + mg\sin\varphi\cos\Theta \\ F_z &= m(\dot{W} - qU + pV) + mg\cos\varphi\cos\Theta \end{aligned} \tag{1}$$

where U, V, W are the speeds along the x, y, and z axes, respectively, m is the mass of the UAV, g is the gravitational constant and the dot over variables denotes time derivative. The final rotation equations are

$$\begin{aligned} M_x &= I_{xx}\dot{p} - (I_{yy} - I_{xx})qr - I_{xz}(pq + \dot{r}) \\ M_y &= I_{yy}\dot{q} - (I_{zz} - I_{xx})pr + I_{xz}(p^2 - r^2) \\ M_z &= I_{zz}\dot{r} - (I_{xx} - I_{yy})qp - I_{xz}(\dot{p} - rq) \end{aligned} \tag{2}$$

where I_{xx}, I_{yy}, I_{zz} are the UAV body inertial parameters along the three axes.

Fig. 1 shows the target localization system of each UAV. With the influences of UAV 6-DOF dynamic model, we need to translate the next waypoint commands into UAV dynamic changes in the UAV path optimization algorithm.

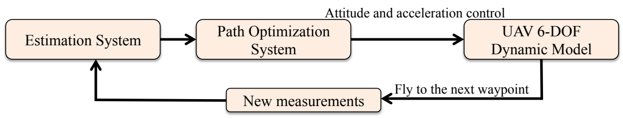

Fig. 1. Target localization system of each UAV.

3. DIFFUSION EXTENDED KALMAN FILTER FOR AOA TARGET LOCALIZATION

This paper focuses on 2D AOA target localization with multiple UAVs. Every mobile UAV can get its own estimate by using different angle measurements. The target localization geometry for a single UAV is depicted in Fig. 2.

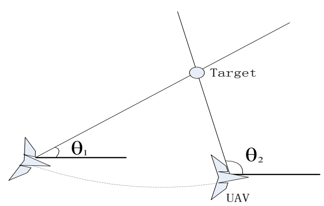

Fig. 2. AOA target localization geometry for a single mobile UAV.

The angle measurement model is given by:

$$\theta_{i,k} = \arctan \frac{y_e - y_{i,k}}{x_e - x_{i,k}}, \quad -\pi < \theta_k \leq \pi \tag{3}$$

where $[x_e, y_e]$ and $[x_{i,k}, y_{i,k}]$ are the stationary target and the ith UAV locations at time k, respectively.

The distributed UAV target localization method is comprised of two phases; namely, distributed estimation and distributed UAV path optimization. This section introduces the distributed estimation algorithm. The UAVs sharing their information are called neighboring UAVs. Here we use l to represent the neighboring UAVs. The target state is defined as

$$\boldsymbol{x}_k = [x_e, \dot{x}_e, y_e, \dot{y}_e]^T \tag{4}$$

where $[\dot{x}_e, \dot{y}_e]$ are the target velocities and ^{T} denotes matrix transpose. The AOA measurement model at time k can be written as

$$z_{i,k} = \theta_{i,k} + n_{i,k} \tag{5}$$

where $n_{i,k}$ is the additive zero-mean Gaussian white noise at time k with variance $R_{i,k}$ which is assumed to depend on the target range [4]:

$$R_{i,k} = \sigma_u^2 d_{i,k}^{\gamma}. \tag{6}$$

Here σ_u^2 is the unit distance noise variance, $d_{i,k}$ is the distance between the ith UAV and the target, and γ is the power loss exponent. The target kinematic model is given by

$$\boldsymbol{x}_k = \boldsymbol{F}_{k-1}\boldsymbol{x}_{k-1}, \quad \boldsymbol{F}_{k-1} = \begin{bmatrix} 1 & T & 0 & 0 \\ 0 & 1 & 0 & 0 \\ 0 & 0 & 1 & T \\ 0 & 0 & 0 & 1 \end{bmatrix} \tag{7}$$

where T is the time interval between discrete-time measurements.

In this paper we assume a constant-velocity target. Extension to manuevering targets is straightforward. Based on the diffusion Kalman filter and EKF [14, 15], we develop a diffusion extended Kalman filter (DEKF) algorithm. It includes three steps. First, the incremental update is given by

$$\begin{aligned} &\boldsymbol{x}_{i,k|k-1} = \boldsymbol{F}_{k-1}\boldsymbol{x}_{i,k-1|k-1} \\ &\boldsymbol{P}_{i,k|k-1} = \boldsymbol{F}_{k-1}\boldsymbol{P}_{i,k-1|k-1}\boldsymbol{F}_{k-1}^T \\ &\boldsymbol{\psi}_{i,k} \leftarrow \boldsymbol{x}_{i,k|k-1} \\ &\boldsymbol{P}_{i,k} \leftarrow \boldsymbol{P}_{i,k|k-1}. \end{aligned} \tag{8}$$

Second, to update the estimate and covariance matrix, the information of every neighboring UAV l (including the ith UAV itself) is needed

$$\begin{aligned} &z_{l,k} = \theta_{l,k} + n_{l,k} \\ &h(\boldsymbol{x}_{l,k|k}) = \arctan\left(\tfrac{\Delta y}{\Delta x}\right) \\ &\boldsymbol{H}_{l,k} = \tfrac{\partial h(\boldsymbol{x}_{l,k|k})}{\partial \boldsymbol{x}_{l,k|k}} \\ &R_e \leftarrow R_{l,k} + \boldsymbol{H}_{l,k}\boldsymbol{P}_{i,k}\boldsymbol{H}_{l,k}^T \\ &\boldsymbol{\psi}_{i,k} \leftarrow \boldsymbol{\psi}_{i,k} + \boldsymbol{P}_{i,k}\boldsymbol{H}_{l,k}^T R_e^{-1}[z_{l,k} - \boldsymbol{H}_{l,k}\boldsymbol{\psi}_{i,k}] \\ &\boldsymbol{P}_{i,k} \leftarrow \boldsymbol{P}_{i,k} - \boldsymbol{P}_{i,k}\boldsymbol{H}_{l,k}^T R_e^{-1}\boldsymbol{H}_{l,k}\boldsymbol{P}_{i,k} \end{aligned} \tag{9}$$

where $\Delta y = \hat{y}_{e,k|k-1} - y_{l,k}$, $\Delta x = \hat{x}_{e,k|k-1} - x_{l,k}$ ($\hat{}$ refers to estimation result) and $\boldsymbol{H}_{l,k}$ is the 1×4 Jacobian of $h(\boldsymbol{x}_{l,k|k})$. Third, combine the results

$$\begin{aligned} &\boldsymbol{x}_{i,k|k} \leftarrow \sum_{l=1}^{N} c_{l,k}\boldsymbol{\psi}_{l,k} \\ &\boldsymbol{P}_{i,k|k} \leftarrow \boldsymbol{P}_{i,k} \end{aligned} \tag{10}$$

where $\boldsymbol{x}_{i,k|k}$ means the target state estimated by the ith UAV, N is the number of the neighboring UAVs, $\leftarrow$ means a parallel and sequential process and $c_{l,k}$ is the diffusion weight of each neighboring UAV at time k. The sum of $c_{l,k}$ equals one [14]. Here we use the inverse trace of every UAV's estimation covariance matrix as the weights. For the ith UAV, the weights of its neighboring UAVs are

$$a_{m,k} = \frac{1}{\mathrm{tr}(\boldsymbol{P}_{m,k|k})} \tag{11a}$$

$$c_{l,k} = \frac{a_{l,k}}{\sum\limits_{m=1}^{N} a_{m,k}}. \tag{11b}$$

As different UAVs have different N, the $c_{l,k}$ will be different. All UAVs calculate their own estimates first and then improve them using the information from their neighbors.

Each UAV in the distributed strategy can get their neighbors' Jacobian vectors $\boldsymbol{H}_{l,k}$ and state estimation results. There is no long distance communication cost between UAVs and a command center. Besides, every UAV is independent and robust to link failures. In the centralized method, all UAVs will need to send their information back to a command center and wait for the updated next waypoint commands. In the next section we will introduce the distributed UAV path optimization method.

4. DISTRIBUTED PATH OPTIMIZATION

In order to improve localization performance, distributed UAV path optimization based on gradient descent method is proposed. In the centralized strategy [4], the cost function in path optimization is designed without considering the influences of information sharing between different UAVs. However, in distributed UAV path optimization, the algorithm complexity will increase because of the impacts of information sharing. Our main task is to design a distributed algorithm considering the information sharing. In addition, different UAVs have different information sharing networks.

The mean squared error (MSE) is used to evaluate the estimation performance. The objective of UAV path optimization is to minimize the MSE. First we define the path optimization cost function of each UAV as:

$$J(\boldsymbol{u}_{i,k}) = \mathrm{tr}(\boldsymbol{P}_{i,k|k}) \tag{12}$$

where $\mathrm{tr}(\boldsymbol{P}_{i,k|k})$ is the trace of state estimate covariance matrix for the ith UAV from (8), and $\boldsymbol{u}_{i,k} = [x_{i,k}, y_{i,k}]^T$ is the ith UAV location at time k. In gradient-descent optimization, the next waypoint $\boldsymbol{u}_{i,k+1}$ should satisfy the relationship [4]

$$\boldsymbol{u}_{i,k+1} - \boldsymbol{u}_{i,k} = -vT \frac{\frac{\partial J(\boldsymbol{u}_{i,k})}{\partial \boldsymbol{u}_{i,k}}}{\left\| \frac{\partial J(\boldsymbol{u}_{i,k})}{\partial \boldsymbol{u}_{i,k}} \right\|}. \tag{13}$$

For the ith UAV, the gradient vector can be numerically calculated using finite-difference approximation of derivatives:

$$\frac{\partial J(\boldsymbol{u}_{i,k})}{\partial \boldsymbol{u}_{i,k}} \approx \begin{bmatrix} \frac{J([x_{i,k}+\delta, y_{i,k}]) - J(\boldsymbol{u}_{i,k})}{\delta} \\ \frac{J([x_{i,k}, y_{i,k}+\delta]) - J(\boldsymbol{u}_{i,k})}{\delta} \end{bmatrix} \tag{14}$$

where δ is the distance to the next waypoint. If δ is chosen small, the gradient will depend on the local information. To compute (14), we need to re-calculate $J([x_{i,k}+\delta, y_{i,k}])$ and $J([x_{i,k}, y_{i,k}+\delta])$. Defining

$$\begin{aligned} h_x(\boldsymbol{x}_{i,k|k}) &= \arctan\left(\frac{\Delta y}{\Delta x + \delta}\right) \\ h_y(\boldsymbol{x}_{i,k|k}) &= \arctan\left(\frac{\Delta y + \delta}{\Delta x}\right) \end{aligned} \tag{15}$$

and substituting the Jacobian matrices of $h_x(\boldsymbol{x}_{i,k|k})$ and $h_y(\boldsymbol{x}_{i,k|k})$ into (9), we get

$$\begin{aligned} &\boldsymbol{H}_{i,k} = \frac{\partial h_x(\boldsymbol{x}_{i,k|k})}{\partial \boldsymbol{x}_{i,k|k}} \quad \text{or} \quad \frac{\partial h_y(\boldsymbol{x}_{i,k|k})}{\partial \boldsymbol{x}_{i,k|k}} \\ &R_e \leftarrow R_{l,k} + \boldsymbol{H}_{l,k}\boldsymbol{P}_{i,k}\boldsymbol{H}_{l,k}^T \\ &\boldsymbol{P}_{i,k} \leftarrow \boldsymbol{P}_{i,k} - \boldsymbol{P}_{i,k}\boldsymbol{H}_{l,k}^T R_e^{-1} \boldsymbol{H}_{l,k}\boldsymbol{P}_{i,k}. \end{aligned} \tag{16}$$

From (16), we obtain two new covariance matrices $\boldsymbol{P}_{i,k}$ and $\boldsymbol{P}_{i,k}^{'}$ for $h_x(\boldsymbol{x}_{i,k|k})$ and $h_y(\boldsymbol{x}_{i,k+1|k})$, respectively. Note that only the ith UAV's $\boldsymbol{H}_{i,k}$ is updated in the above computations while other neighboring UAVs retain their $\boldsymbol{H}_{i,k}$ unchanged. The new cost function values are given by

$$\begin{aligned} J([x_{i,k}+\delta, y_{i,k}]) &= \mathrm{tr}(\boldsymbol{P}_{i,k+1}) \\ J([x_{i,k}, y_{i,k}+\delta]) &= \mathrm{tr}(\boldsymbol{P}_{i,k+1}^{'}). \end{aligned} \tag{17}$$

Using normalization, the next waypoint for the ith UAV is obtained from

$$\boldsymbol{u}_{i,k+1} = \boldsymbol{u}_{i,k} - vT \frac{\frac{\partial J(\boldsymbol{u}_{i,k})}{\partial \boldsymbol{u}_{i,k}}}{\left\| \frac{\partial J(\boldsymbol{u}_{i,k})}{\partial \boldsymbol{u}_{i,k}} \right\|} \tag{18}$$

where $\|\cdot\|$ denotes the Euclidean norm.

For each UAV, an optimal path for MSE reduction can be acquired by using this path optimization algorithm. However, the optimal paths and estimation performance of different UAVs significantly depend on their own communication network. The communication topology will be analyzed in next section.

5. DYNAMIC COMMUNICATION TOPOLOGY AND COMPLEXITY

Communication topology examples of the normal centralized and distributed strategies are shown in Fig. 5. The directions of the information delivered are indicated by the arrows. From Fig. 5(a), a command center is necessary and only one communication topology mode exists in the centralized strategy. However, in the distributed strategy, there is no command center and different UAVs have different communication networks.

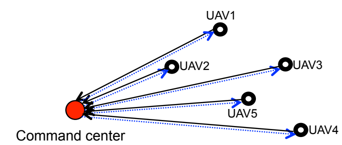

(a)

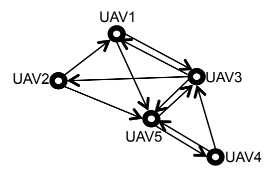

(b)

Fig. 3. Schematic diagram of UAVs communication topology: (a) centralized strategy, (b) distributed strategy.

In practical applications, each UAV has a communication range constraint and thus if the UAVs are very far from each other they cannot share information until they get close enough. Therefore, different UAVs have different dynamic communication topologies. In this paper, we consider the distributed UAV target localization system has a dynamic communication topology. Fig. 4 shows the details of the topology change process.

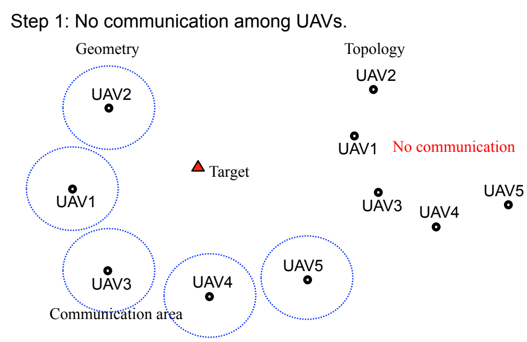

(a)

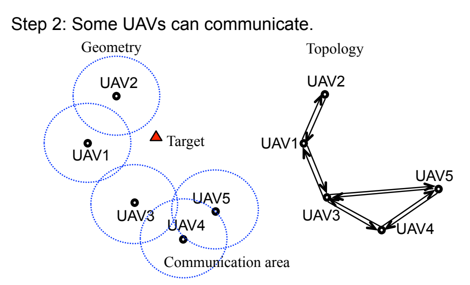

(b)

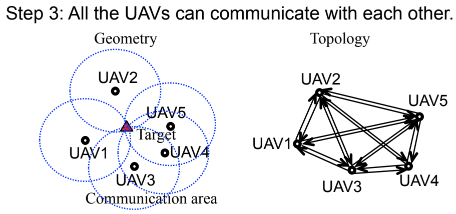

(c)

Fig. 4. Schematic diagram of the dynamic communication topology: (a) Step 1, (b) Step 2, (c) Step 3.

In the centralized strategy (Fig. 5(a)), the information on one arrow contains a measurement angle or an updated UAV next waypoint 1×2 vector. Then, the communications between each UAV and the command center are $1 + 2 = 3$. In the distributed strategy, the $\boldsymbol{H}_{l,k}$ is a 1×4 vector and the estimate $\boldsymbol{x}_{i,k|k}$ is a 1×4 vector. The neighboring UAVs will share the measurement that only contains 1×1 information. The trace of the covariance matrix, a 1×1 data, will be sent from the neighboring UAVs as well. Thus, the communications would be $1 \times 4 + 1 \times 4 + 1 + 1 = 10$ on one arrow. The total communication information in the distributed strategy is larger than that in the centralized one. But the communication energy cost between the far away command center and UAVs is huge. Thus, from the aspect of communication energy cost, the proposed distributed strategy has a significant advantage.

6. SIMULATION STUDIES

In this section, we compare the performance of our proposed distributed strategy with a centralized strategy. The centralized method uses an EKF as the estimator. The UAVs' initial positions are $[-400, -500]$ m, $[-200, 2000]$ m, $[500, -600]$ m, $[1900, -200]$ m and $[-500, 600]$ m. A stationary target is at $[1000, 1000]$ m with a circular no fly zone of radius 180 m centered about the target. All the UAVs have the same initial state matrix $X_{0|0} = [1300, 0, 700, 0]^T$ and covariance matrix $P_{0|0} = \text{diag}[3000, 0, 3000, 0]$. The simulation runs for 100 sampling points with 2-second time intervals. The measurement noise is $\sigma = 1^o$ per meter with $\gamma = 0.2$ power loss exponent and $\delta = 200$. The communication range constraint is 700 m. The UAVs' fly speed is 30 m/s. A UAV 6-DOF dynamic model is built in Simulink and the parameters are from [13] with a proportional-integral-derivative (PID) controller. To evaluate the estimation performance, mean squared errors (MSEs) are calculated by the trace of the covariance matrix in the DEKF. Note that the MSEs applied here can evaluate the performance of different methods properly but they are not the exact values of the state estimates [10]. The averaged-MSE is calculated from the 5 UAVs' MSEs. Collision avoidance problem is ignored in this paper.

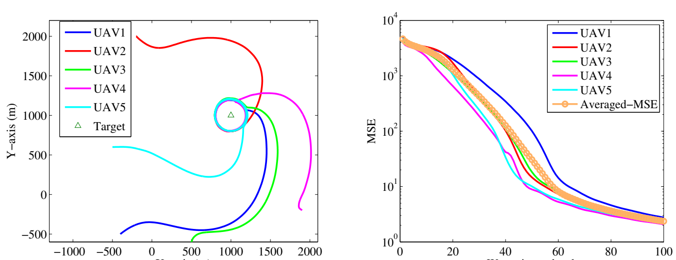

(a) (b)

Fig. 5. (a) Optimal UAV trajectories using 5 independent UAVs, (b) MSE performance comparison.

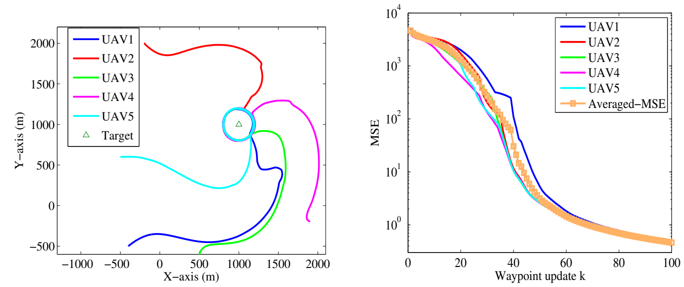

(a) (b)

Fig. 6. (a) Optimal UAV trajectories using proposed distributed method, (b) MSE performance.

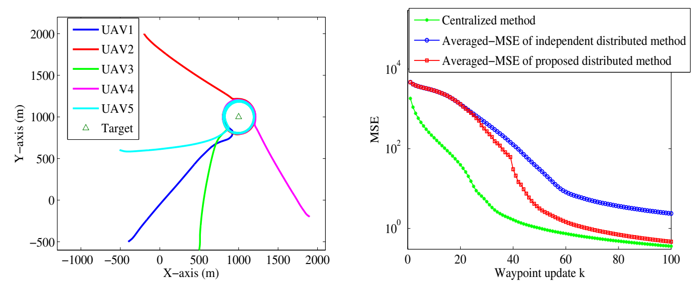

(a) (b)

Fig. 7. (a) Optimal UAV trajectories using centralized method, (b) MSE performance comparison.

Fig. 5 shows the trajectories of using 5 independent UAVs (never share information with each other) and MSE performance. Fig. 6 shows the results of using the method developed in this paper. The results of using the centralized strategy are shown in Fig. 7. The MSE comparison among the independent, proposed distributed and centralized strategies is in Fig. 7(b). As introduced in Section 5, in distributed strategies, the 5 UAVs cannot share information at beginning. So the trajectories are similar to those in Fig. 5. As the UAVs get closer with each other, some of them can share information and the estimation performance is improved significantly. The trajectories begin to change. Finally, all the UAVs can communicate with each other and thus the communication topology becomes a centralized mode. From Fig. 7(b), the performance of the proposed distributed method (final averaged-MSE is 0.464) can reach very close to the centralized one (final MSE is 0.357) that is much better than the independent distributed method (final averaged-MSE is 2.364).

7. CONCLUSION

In this paper, we have investigated the problem of distributed UAV path optimization for AOA target localization. We designed a DEKF combined with distributed UAV gradient-descent path optimization algorithm. The distributed UAV path optimization strategy aiming to minimize the trace of the estimation error covariance was proposed. The information sharing restriction in distributed strategy was considered. The UAV 6-DOF was taken into consideration to generate realistic UAV trajectories. The properties and effectiveness of the proposed method have been discussed and verified by simulation examples. The future work will consider using multiple UAVs with distributed path optimization to track a moving target in 3D space.

8. REFERENCES

[1] M. Gavish and A.J. Weiss, "Performance analysis of bearing-only target location algorithms," *IEEE Trans. Aerosp. Electron. Syst.*, vol. 28, no. 3, pp. 817–828, Jul 1992.

[2] Y. Bar-Shalom, *Multitarget-multisensor tracking: Applications and advances. Volume III*, 2000.

[3] J.A. Fawcett, "Effect of course maneuvers on bearings-only range estimation," *IEEE Trans. Acoust., Speech, Signal Process.*, vol. 36, no. 8, pp. 1193–1199, Aug 1988.

[4] K. Dogancay, "Single- and multi-platform constrained sensor path optimization for angle-of-arrival target tracking," in *Signal Processing Conference, 2010 18th European*, Aug 2010, pp. 835–839.

[5] Y. Oshman and P. Davidson, "Optimization of observer trajectories for bearings-only target localization," *IEEE Trans. Aerosp. Electron. Syst.*, vol. 35, no. 3, pp. 892–902, 1999.

[6] K. Doğançay, "UAV path planning for passive emitter localization," *IEEE Trans. Aerosp. and Electron. Syst.*, vol. 48, no. 2, pp. 1150–1166, 2012.

[7] K. Doğançay and H. Hmam, "Optimal angular sensor separation for AOA localization," *Signal Process.*, vol. 88, no. 5, pp. 1248–1260, 2008.

[8] S.Y. Zhao, B.M. Chen, and T.H. Lee, "Optimal sensor placement for target localization and tracking in 2D and 3D," *Int. J. Control*, vol. 86, no. 10, pp. 1687–1704, 2013.

[9] S. Xu and K. Doğançay, "Optimal sensor deployment for 3D AOA target localization," in *Acoustics, Speech and Signal Processing (ICASSP), 2015 IEEE International Conference on*. IEEE, 2015, pp. 2544–2548.

[10] F.S. Cattivelli and A.H. Sayed, "Diffusion strategies for distributed Kalman filtering and smoothing," *IEEE Trans. Autom. Control*, vol. 55, no. 9, pp. 2069–2084, 2010.

[11] R. Olfati-Saber, "Distributed Kalman filtering for sensor networks," in *Decision and Control, 2007 46th IEEE Conference on*. IEEE, 2007, pp. 5492–5498.

[12] N.H. Nguyen, K. Dogancay, and L.M. Davis, "Adaptive waveform scheduling for target tracking in clutter by multistatic radar system," in *in Proc. Int. Conf. Acoust, Speech, Signal Process.* IEEE, 2014, pp. 1449–1453.

[13] S.M. Calhoun, *Six Degree-of-Freedom Modeling of an Uninhabited Aerial Vehicle*, Ph.D. thesis, Ohio University, 2006.

[14] F. Cattivelli and A.H. Sayed, "Diffusion distributed Kalman filtering with adaptive weights," in *Signals, Systems and Computers, 2009 Conference Record of the Forty-Third Asilomar Conference on*. IEEE, 2009, pp. 908–912.

[15] K. Spingarn, "Passive position location estimation using the extended Kalman filter," *IEEE Trans. Aerosp. Electron. Syst.*, vol. AES-23, no. 4, pp. 558–567, July 1987.